

# <sup>1</sup>H and <sup>79</sup>Br NMR in 1,4-Didecyl-1,4-diazoniabicyclo[2.2.2]octane Dibromide and Diiodide

Hirokazu NAKAYAMA,<sup>†</sup> Taro EGUCHI,<sup>†</sup> Nobuo NAKAMURA, Hideaki CHIHARA,\* Takashi NOGAMI,<sup>††</sup>  
Kengo IMAMURA,<sup>††</sup> and Yasuhiko SHIROTA<sup>††</sup>

Department of Chemistry, Faculty of Science, Osaka University, Toyonaka, Osaka 560

<sup>†</sup>Institute of Chemistry, College of General Education, Osaka University, Toyonaka, Osaka 560

<sup>††</sup>Department of Applied Chemistry, Faculty of Engineering, Osaka University, Yamada-oka, Suita, Osaka 565  
(Received August 25, 1988)

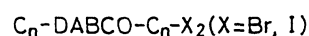
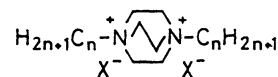
Temperature dependence of <sup>1</sup>H NMR spin-lattice relaxation time was measured in solid 1,4-didecyl-1,4-diazoniabicyclo[2.2.2]octane dibromide and diiodide (C<sub>10</sub>-DABCO-C<sub>10</sub>-Br<sub>2</sub> and C<sub>10</sub>-DABCO-C<sub>10</sub>-I<sub>2</sub>). <sup>79</sup>Br NMR spin-lattice relaxation time and chemical shift measurements in the high-temperature phase were also performed in C<sub>10</sub>-DABCO-C<sub>10</sub>-Br<sub>2</sub>. It was found that the cation rotates isotropically, while the anion diffuses at a correlation time of ca. 10<sup>-8</sup> s in the high-temperature phase of C<sub>10</sub>-DABCO-C<sub>10</sub>-Br<sub>2</sub>. The activation energies for these modes are 30 and 34 kJ mol<sup>-1</sup>, respectively. Methyl reorientation is activated in the low-temperature phase (E<sub>a</sub>=11.8 kJ mol<sup>-1</sup> in C<sub>10</sub>-DABCO-C<sub>10</sub>-Br<sub>2</sub> and E<sub>a</sub>=12.0 kJ mol<sup>-1</sup> in C<sub>10</sub>-DABCO-C<sub>10</sub>-I<sub>2</sub>). Near the phase-transition temperature some motion of decyl chain is observed (E<sub>a</sub>=57 kJ mol<sup>-1</sup> in C<sub>10</sub>-DABCO-C<sub>10</sub>-Br<sub>2</sub> and E<sub>a</sub>=35.5 kJ mol<sup>-1</sup> in C<sub>10</sub>-DABCO-C<sub>10</sub>-I<sub>2</sub>).

A series of symmetric bis(quaternary alkyl halide) salts of 1,4-diazabicyclo[2.2.2]octanes (DABCO) exhibit first order solid-solid phase transitions above room temperature.<sup>1,2)</sup> For these compounds the halide anion conductivities in the high-temperature phases are higher than those in the room-temperature phases by two or three orders of magnitude.<sup>1,2)</sup> This characteristic phase transition has been studied extensively by DSC, IR, and powder X-ray diffraction.<sup>1,2)</sup> It was revealed that the longer the alkyl chain, the higher the transition temperature becomes in both bromide and iodide salts. If the carbon number of alkyl groups is the same, the transition temperature rises in the order of chloride, bromide, and iodide. Temperature dependence of the IR spectra shows abrupt disappearance of the band progressions<sup>1)</sup> above the transition temperatures. These results indicate that the phase transition is accompanied by a conformational change of the alkyl chains. In the case of the unsymmetric bis(quaternary alkyl halide) salts of 1,4-diazabicyclo[2.2.2]octanes, similar phase transitions have been observed.<sup>3,4)</sup>

The conductivities of these compounds are of the order of 10<sup>-5</sup> (Ω cm)<sup>-1</sup> in the high-temperature phases, being considerably low compared with typical super-ionic conductors in which conductivities of the order of 10<sup>-1</sup> to 10<sup>-3</sup> (Ω cm)<sup>-1</sup> have been observed. However, they possess the characteristic feature which is not seen in the other ionic conductors, i.e., the conductivity as well as the transition temperature to the conductive phase can be controlled by changing the length and the assortment of side alkyl chains. Therefore, the compounds of DABCO series are potential candidates of new type of electrical conductors which possess highly controllable characteristics. The extensive works on this series will thus open a new area of the molecular design.

Although we have been engaged in a number of experimental work as mentioned above, the micro-

scopic mechanisms of the phase transitions and of the high electrical conduction in the high-temperature phases of DABCO series compounds have not yet been clarified. In order to shed light upon these points, we conducted measurements of <sup>1</sup>H NMR spin-lattice relaxation times in 1,4-didecyl-1,4-diazoniabicyclo[2.2.2]octane dibromide (C<sub>10</sub>-DABCO-C<sub>10</sub>-Br<sub>2</sub>) and 1,4-didecyl-1,4-diazoniabicyclo[2.2.2]octane diiodide (C<sub>10</sub>-DABCO-C<sub>10</sub>-I<sub>2</sub>), and <sup>79</sup>Br NMR spin-lattice relaxation times and chemical shift in C<sub>10</sub>-DABCO-C<sub>10</sub>-Br<sub>2</sub>.



## Experimental

C<sub>10</sub>-DABCO-C<sub>10</sub>-Br<sub>2</sub> and C<sub>10</sub>-DABCO-C<sub>10</sub>-I<sub>2</sub> were synthesized by the method described in a previous paper.<sup>1)</sup> <sup>1</sup>H NMR spin-lattice relaxation times (T<sub>1</sub>) were measured with the saturation-τ-π/2 pulse sequence by a MATEC pulsed spectrometer between 77 and 400 K. The resonance frequencies were 20.5 MHz for C<sub>10</sub>-DABCO-C<sub>10</sub>-Br<sub>2</sub> and 19.5 MHz for C<sub>10</sub>-DABCO-C<sub>10</sub>-I<sub>2</sub>.

The specimen was sealed in a glass ampoule with a small amount of helium gas for heat exchange. The sample temperatures were measured with Chromel-P-Constantan thermocouples and controlled to within 0.1 K during each run.

<sup>79</sup>Br NMR spin-lattice relaxation time (T<sub>1</sub>) and line shape measurements were carried out by a MATEC pulsed spectrometer with a wide-bore (130 mmφ) Oxford superconducting magnet (4.72 T). The sample temperature was regulated by using a home-made cryostat of liquid flow type. T<sub>1</sub> was measured after 256 signal accumulation by using the saturation-τ-π/2 pulse sequence. The line shape was determined by the Fourier transformation after the 1024 accumulation of FID signals (sampling interval=2 μs and sampling points=2048). The aqueous solution of NaBr and powder NaBr

were used as standard reagents of  $^{79}\text{Br}$  NMR.

### Results and Discussion

Temperature dependence of  $^1\text{H}$  NMR spin-lattice relaxation times ( $T_1$ ) for both compounds is shown in Fig. 1.  $T_1$ 's change abruptly at 337 K in  $\text{C}_{10}\text{-DABCO-C}_{10}\text{-Br}_2$  and at 361 K in  $\text{C}_{10}\text{-DABCO-C}_{10}\text{-I}_2$ . These temperatures agree well with the transition temperatures determined by DSC within the experimental error.<sup>1,2)</sup>

The  $T_1$  minima around 150 K are attributed to reorientation of terminal methyl groups for the following reasons. The spin-lattice relaxation rate due to methyl reorientation is expressed<sup>5)</sup> by

$$T_1^{-1} = A \cdot B(\omega_0 \cdot \tau_c) \omega_0^{-1},$$

where

$$A = -\frac{3}{5} \gamma^4 \hbar^2 r^{-6} I(I+1),$$

$$B(\omega_0 \cdot \tau_c) = \frac{\omega_0 \cdot \tau_c}{1 + (\omega_0 \cdot \tau_c)^2} + \frac{4\omega_0 \cdot \tau_c}{1 + 4(\omega_0 \cdot \tau_c)^2},$$

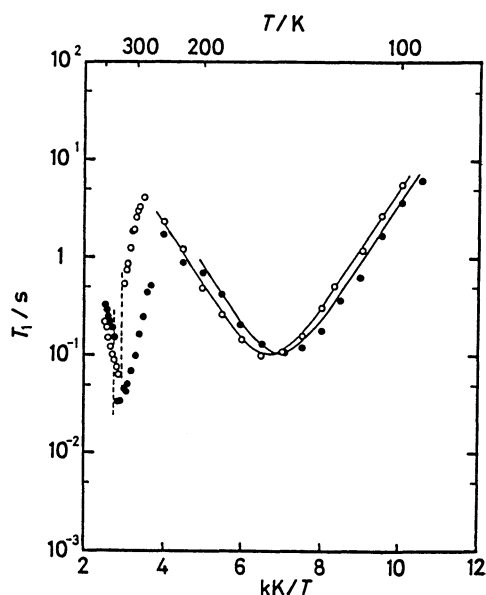


Fig. 1. Temperature dependence of  $^1\text{H}$  NMR spin-lattice relaxation times ( $T_1$ ) in  $\text{C}_{10}\text{-DABCO-C}_{10}\text{-Br}_2$  (○) and  $\text{C}_{10}\text{-DABCO-C}_{10}\text{-I}_2$  (●). The measuring frequencies are 20.5 and 19.5 MHz for  $\text{C}_{10}\text{-DABCO-C}_{10}\text{-Br}_2$  and  $\text{C}_{10}\text{-DABCO-C}_{10}\text{-I}_2$ , respectively. Solid lines are the theoretical curves by assuming the methyl reorientations. The phase-transition temperatures are indicated by vertical broken lines.

and

$$\tau_c = \tau_0 \exp(E_a/kT)$$

where  $\omega_0$  is the nuclear Larmor frequency,  $\tau_c$  is the correlation time,  $r$  is the interproton distance within the methyl group,  $I$  is the spin quantum number, and  $E_a$  is the activation energy. Using  $A$  as an adjustable parameter, we can reproduce  $T_1$  as shown in Fig. 1. The activation energies obtained are given in Table 1. According to the BPP theory,<sup>5)</sup> the methyl reorientation contributes to  $A$  by an amount of  $8.9 \times 10^8 \text{ s}^{-2}$  assuming that all methylene protons are rigid and do not undergo any relaxation, and that the spin-temperature approximation holds in the present system. This value agrees very well with the experimental ones ( $8.5 \times 10^8 \text{ s}^{-2}$  in  $\text{C}_{10}\text{-DABCO-C}_{10}\text{-Br}_2$  and  $8.0 \times 10^8 \text{ s}^{-2}$  in  $\text{C}_{10}\text{-DABCO-C}_{10}\text{-I}_2$ ). We found also that the above experimental results satisfy well an empirical relation between  $E_a$  and the temperature at which  $T_1$  minimum occurs<sup>6)</sup> for both compounds. The  $T_1$  minima around 150 K are, therefore, attributed to the terminal methyl group reorientation.

Temperature dependence of  $T_1$  near the phase-transition temperature is shown in Fig. 2. In the low-

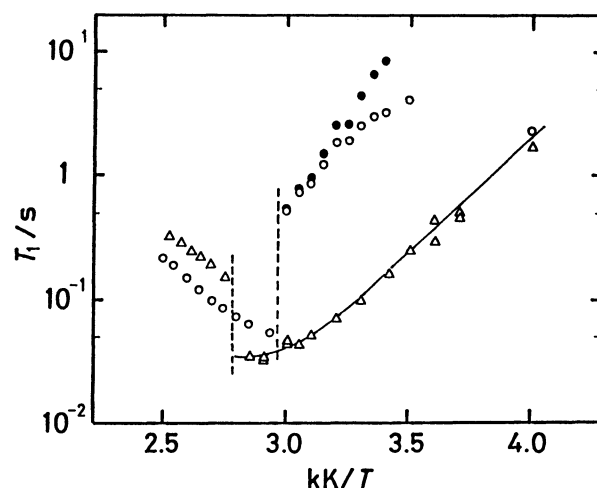


Fig. 2. Temperature dependence of  $^1\text{H}$  NMR spin-lattice relaxation times ( $T_1$ ) near the phase-transition temperatures in  $\text{C}_{10}\text{-DABCO-C}_{10}\text{-Br}_2$  (○) and  $\text{C}_{10}\text{-DABCO-C}_{10}\text{-I}_2$  (△). For  $\text{C}_{10}\text{-DABCO-C}_{10}\text{-Br}_2$   $T_1$  is contributed by the methyl reorientation and another undefined mode (●). The measuring frequencies are 20.5 and 19.5 MHz for  $\text{C}_{10}\text{-DABCO-C}_{10}\text{-Br}_2$  and  $\text{C}_{10}\text{-DABCO-C}_{10}\text{-I}_2$ , respectively.

Table 1. Activation Energies in  $\text{C}_{10}\text{-DABCO-C}_{10}\text{-Br}_2$  and  $\text{C}_{10}\text{-DABCO-C}_{10}\text{-I}_2$

	Low-temperature phase		High-temperature phase
	$\text{CH}_3$ rotation	Large angle oscillation?	Overall rotation
	$E_a/\text{kJ mol}^{-1}$	$E_a/\text{kJ mol}^{-1}$	$E_a/\text{kJ mol}^{-1}$
$\text{C}_{10}\text{-DABCO-C}_{10}\text{-I}_2$	12.0	35.5	28.0
$\text{C}_{10}\text{-DABCO-C}_{10}\text{-Br}_2$	11.8	57	30

temperature phase near the phase-transition point, the  $T_1$  decreases with increasing temperature. For  $\text{C}_{10}\text{-DABCO-C}_{10}\text{-Br}_2$   $T_1$  is contributed by two components in this temperature region. One is the contribution of methyl reorientation mentioned above. The other component discussed here is also shown in Fig. 2 as solid circles. The mechanism of this relaxation can not be pinned down at present stage: A large angle oscillation of the decyl chain is the most probable candidate. The activation energies for this mode are  $57 \text{ kJ mol}^{-1}$  for  $\text{C}_{10}\text{-DABCO-C}_{10}\text{-Br}_2$  and  $35.5 \text{ kJ mol}^{-1}$  for  $\text{C}_{10}\text{-DABCO-C}_{10}\text{-I}_2$ . In the high-temperature phases, the  $T_1$ 's become longer with increasing temperature with apparent activation energies of  $30 \text{ kJ mol}^{-1}$  for  $\text{C}_{10}\text{-DABCO-C}_{10}\text{-Br}_2$  and  $28 \text{ kJ mol}^{-1}$  for  $\text{C}_{10}\text{-DABCO-C}_{10}\text{-I}_2$ . The free induction decays (FID) are shown in Fig. 3 where  $T_2^* = 33 \mu\text{s}$  in the high-temperature phase in comparison with  $T_2^* = 8 \mu\text{s}$  in the room-temperature phase. In the high-temperature phase the line widths, which are equal to the inverse of  $T_2^*$ , are relatively wide and comparable with those often encountered in liquid crystalline phase or plastic phase. In addition, the polarizing microscope study<sup>1)</sup> gave an evidence that the high-temperature phase is isotropic. The IR spectra showed that the ordered trans-zigzag conformation of the alkyl chain is lost in the high-temperature phase.<sup>2)</sup> All these facts suggest that overall rotation of the cation is excited in the high-temperature phase.

In the high-temperature phase, the activation energies for these two compounds are almost the same. This fact suggests strongly that the cations in both materials are in similar environment. On the other hand, the activation energy for large-amplitude motion in the low-temperature phase is significantly lower in  $\text{C}_{10}\text{-DABCO-C}_{10}\text{-I}_2$  than in  $\text{C}_{10}\text{-DABCO-C}_{10}\text{-Br}_2$ , due probably to larger void space available to the cations, which is brought about by larger size of

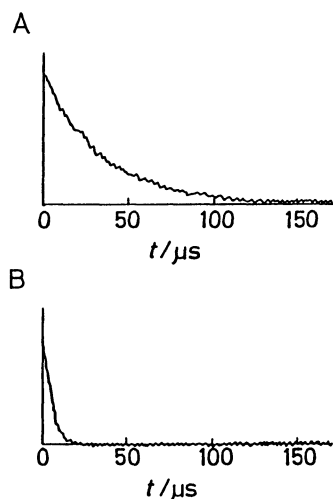


Fig. 3. Free induction decays of  $^1\text{H}$  NMR in  $\text{C}_{10}\text{-DABCO-C}_{10}\text{-Br}_2$  (A) in the high-temperature phase and (B) in the room-temperature phase.

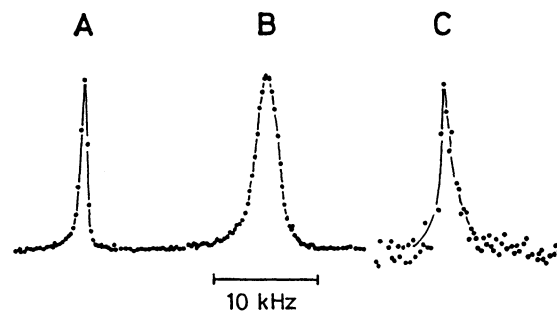


Fig. 4.  $^{79}\text{Br}$  FT-NMR spectra A) in NaBr water solution, B) in NaBr powder, and C) in  $\text{C}_{12}\text{-DABCO-C}_{12}\text{-Br}_2$ .

the anion in the former material. Since the cationic motion is highly excited in  $\text{C}_{10}\text{-DABCO-C}_{10}\text{-I}_2$ , the difference in the Gibbs energy in low- and high-temperature phases is certainly small compared with  $\text{C}_{10}\text{-DABCO-C}_{10}\text{-Br}_2$  and the transition temperature of  $\text{C}_{10}\text{-DABCO-C}_{10}\text{-I}_2$  is significantly higher than that of  $\text{C}_{10}\text{-DABCO-C}_{10}\text{-Br}_2$ .

$^{79}\text{Br}$  NMR of  $\text{C}_n\text{-DABCO-C}_n\text{-Br}_2$  ( $n=10, 12, 14$ ) were observed only in the high-temperature phases. The line shape in  $\text{C}_{12}\text{-DABCO-C}_{12}\text{-Br}_2$  at 363 K is shown in Fig. 4 together with those in aqueous solution of NaBr and powdered NaBr. The line shapes and the line widths in  $\text{C}_{10}\text{-DABCO-C}_{10}\text{-Br}_2$  and  $\text{C}_{14}\text{-DABCO-C}_{14}\text{-Br}_2$  are nearly the same as those in  $\text{C}_{12}\text{-DABCO-C}_{12}\text{-Br}_2$ . In NaBr crystals Br nuclei are located at the sites of cubic symmetry so that the electric field gradient (EFG) at the Br site vanishes. Hence one expects neither first order splitting nor second order shift of the  $^{79}\text{Br}$  resonance in NaBr. The finite line width in this compound shown in Fig. 4 is due probably to imperfection of the crystal lattice and to the magnetic dipole interaction which can be hardly estimated because of the lack of the crystal-structure data. The resonance frequency in NaBr crystals coincides with that in aqueous solution of NaBr listed in Table 2. The line width in  $\text{C}_n\text{-DABCO-C}_n\text{-Br}_2$  (Fig. 4) is narrower than that in powdered NaBr, indicating that the EFG at the Br site vanishes and moreover, any extrinsic EFG due to lattice imperfection and magnetic dipole interaction are averaged out due to rapid translational diffusion of  $\text{Br}^-$  as will be discussed later. In the low-temperature phases the  $^{79}\text{Br}$  NMR could not be observed due to large quadrupolar line broadening. The most remarkable point in Table 2 is that  $\text{C}_n\text{-DABCO-C}_n\text{-Br}_2$  ( $n=10, 12, \text{ or } 14$ )

Table 2.  $^{79}\text{Br}$  NMR Frequencies, Line Widths, and Chemical Shifts

System	$\nu/\text{MHz}$	$\Delta\nu/\text{kHz}$	$\delta/\text{ppm}$
$\text{C}_n\text{-DABCO-C}_n\text{-Br}_2$ ( $n=10, 12, 14$ )	50.5360	1.5	3660
NaBr powder	50.3517	3.0	0
NaBr solution	50.3517	1.0	0

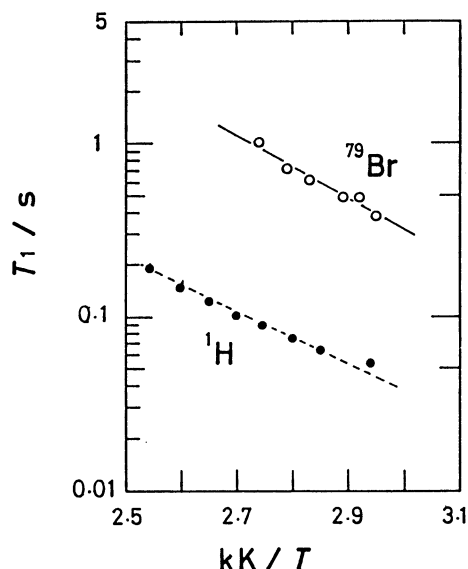


Fig. 5. Temperature dependence of  $^{79}\text{Br}$  (50.5 MHz) and  $^1\text{H}$  NMR (20.5 MHz)  $T_1$ 's in the high-temperature phase of  $\text{C}_{10}\text{-DABCO-C}_{10}\text{-Br}_2$ .

show a very large down-field chemical shift. The interpretation by a second-order quadrupole effect is ruled out because of very narrow, symmetric line shape as shown in Fig. 4. Thus one must consider that there exists some special mechanism to generate a large paramagnetic term in the DABCO series compounds. At present we cannot identify the origin of such a large paramagnetic shift.

The temperature dependence of  $^{79}\text{Br}$  and  $^1\text{H}$   $T_1$ 's in  $\text{C}_{10}\text{-DABCO-C}_{10}\text{-Br}_2$  are shown in Fig. 5.  $^{79}\text{Br}$   $T_1$  is longer than  $^1\text{H}$   $T_1$  by an order of magnitude, and its temperature slope is slightly larger.  $^{79}\text{Br}$   $T_1$  (solid line in Fig. 5) shows that  $\omega_0\tau_c < 1$  and leads to  $E_a = 34 \pm 3$   $\text{kJ mol}^{-1}$  which can be attributed to the translational diffusion of  $\text{Br}^-$  anions. Since the overall rotation of

cations as well as anionic diffusion is highly excited in the isotropic high-temperature phase, this phase can be classified as an ionic plastic crystal.  $\text{NH}_4\text{NO}_3$ ,<sup>7)</sup>  $\text{TlNO}_3$ ,<sup>8)</sup>  $\text{CH}_3\text{NH}_3\text{I}$ <sup>9)</sup> have been considered to belong to this category.

In conclusion, the methyl reorientation is first activated in the low-temperature phase ( $E_a = 11.8$   $\text{kJ mol}^{-1}$  in  $\text{C}_{10}\text{-DABCO-C}_{10}\text{-Br}_2$  and  $E_a = 12.0$   $\text{kJ mol}^{-1}$  in  $\text{C}_{10}\text{-DABCO-C}_{10}\text{-I}_2$ ). On further increase in temperature the large angle oscillation of the decyl chains may govern the relaxation mechanism ( $E_a = 35.5$   $\text{kJ mol}^{-1}$  and 57  $\text{kJ mol}^{-1}$  in  $\text{C}_{10}\text{-DABCO-C}_{10}\text{-I}_2$  and  $\text{C}_{10}\text{-DABCO-C}_{10}\text{-Br}_2$ ). In the high-temperature phase the overall rotation of cations are excited ( $E_a = 28.0$   $\text{kJ mol}^{-1}$  and 30  $\text{kJ mol}^{-1}$  in  $\text{C}_{10}\text{-DABCO-C}_{10}\text{-I}_2$  and  $\text{C}_{10}\text{-DABCO-C}_{10}\text{-Br}_2$ ). Furthermore, the anions diffuse at a rate higher than  $10^8$   $\text{s}^{-1}$  with an activation energy of  $E_a = 34$   $\text{kJ mol}^{-1}$ .

## References

- 1) J. Shimizu, T. Nogami, and H. Mikawa, *Solid State Commun.*, **54**, 1009 (1985).
- 2) J. Shimizu, I. Imamura, T. Nogami, and H. Mikawa, *Bull. Chem. Soc. Jpn.*, **59**, 1443 (1986).
- 3) J. Shimizu, K. Imamura, T. Nogami, and H. Mikawa, *Bull. Chem. Soc. Jpn.*, **59**, 3367 (1986).
- 4) K. Imamura, J. Shimizu, and T. Nogami, *Bull. Chem. Soc. Jpn.*, **59**, 2699 (1986).
- 5) A. Abragam, "The Principles of Nuclear Magnetism," Clarendon Press, Oxford (1961).
- 6) T. Eguchi and H. Chihara, *J. Magn. Reson.*, **76**, 143 (1988).
- 7) M. T. Riggan, R. R. Knispel, and M. M. Pintar, *J. Chem. Phys.*, **56**, 2911 (1972).
- 8) K. Moriya, T. Matsuo, and H. Suga, *J. Phys. Chem. Solids*, **44**, 1103 (1983).
- 9) H. Ishida, R. Ikeda, and D. Nakamura, *Bull. Chem. Soc. Jpn.*, **59**, 915 (1986).